

As₂Se₃ melt crystallization studied by quadratic approximation of nucleation and growth rate temperature dependence

Jozef Chovanec · Mária Chromčíková ·
Petr Pilný · Jana Shánělová · Jiří Málek ·
Marek Liška

Received: 12 December 2012 / Accepted: 19 February 2013 / Published online: 20 March 2013
© Akadémiai Kiadó, Budapest, Hungary 2013

Abstract The constant heating rate crystallization of As₂Se₃ undercooled melt was measured by the differential scanning calorimetry. The nonlinear regression analysis of conversion temperature dependence was performed in frame of the classical nucleation theory supposing the normal 3D growth. The parameters of temperature dependence of nucleation rate and growth rate were determined by three step process. First the simple parabolic model was used to estimate the maximum and width of nucleation/growth rate temperature dependence. Then the obtained parabolic curves were fitted by the theoretical ones. In the third step, the obtained parameters were used as zero estimates for nonlinear regression analysis of experimental data. The results obtained by using conversion degree α were compared with the results obtained by using the $-\ln(1 - \alpha)$ transformed function. Although both treatments give comparable results the use of $-\ln(1 - \alpha)$ input data is preferred due to better numerical stability of nonlinear regression treatment.

Keywords DSC · Nucleation · Crystal growth · Arsenic triselenide

Introduction

Due to high transmittance in the infrared region, low phonon energies, and significant nonlinearity of their optical properties chalcogenide glasses have been the subject of intense fundamental and applied research for a long time [1–4]. The details of non-isothermal crystallization kinetics are currently intensively studied by using various experimental techniques for various systems but with simplified mathematical treatment avoiding the direct integration of kinetic equations for given time–temperature regime [5–11]. Among the properties studied namely the kinetics of crystallization tightly bounded with the glass forming ability plays the crucial role. The nucleation and growth of the As₂Se₃ glass as well as the Raman spectra and glass structure were studied by Holubova et al. [12–15].

In the previous work [15] dealing with the As₂Se₃ crystallization kinetics, the quadratic approximation of nucleation rate, I , and growth rate, u , temperature dependences were proposed. The degree of conversion was determined by remelting of crystallized samples obtained by crystallization experiments with specifically designed time–temperature regimes emphasizing the various time intervals given to the system at temperatures from the temperature region where only the nucleation takes place. In this work, the same procedure of quadratic approximation followed by nonlinear regression with theoretical I and u temperature dependencies is applied to the crystallization data obtained by simple recording of the DTA crystallization peaks measured at two different heating rates preceded with the same isothermal nucleation treatment. Moreover, the attention is paid to the influence of substituting the degree of conversion α by the transformed function $-\ln(1 - \alpha)$.

J. Chovanec (✉) · P. Pilný · J. Shánělová · J. Málek
Department of Physical Chemistry, Faculty of Chemical
Technology, University of Pardubice, 532 10 Pardubice,
Czech Republic
e-mail: jozef.chovanec@upce.cz

M. Chromčíková · M. Liška
Vitrum Laugaricio, Joint Glass Center of IIC SAS, TnU AD,
RONA, and FChPT STU, 911 50 Trenčín, Slovakia

Method

In frame of the classic nucleation theory (CNT), the volume of crystalline phase, V_{cr} , crystallized at time t can be expressed by [3, 16–19]:

$$V_{cr}(t) = g \int_0^t V_{me}(t') I[T(t')] \left\{ \int_{t'}^t u[T(t'')] dt'' \right\}^d dt', \tag{1}$$

where $V_{me}(t')$ represents the volume of liquid phase, and we suppose the congruent crystallization, i.e., the rate of homogeneous nucleation, I , as well as the linear growth rate, u , depend only on the temperature. For low values of the degree of conversion $\alpha = V_{cr}/(V_{me} + V_{cr})$, we can neglect the time dependence of V_{me} and consider it equal to the total system volume $V_{me} \approx V_{me} + V_{cr}$. The exponent d and the shape factor g depend on the crystal shape—for the spherical particles $d = 3$ and $g = 4\pi/3$.

The temperature dependence of the homogeneous nucleation rate can be expressed as:

$$I(T) = N_s \frac{kT}{h} \exp\left(-\frac{\Delta G_a}{kT}\right) N \exp\left[-\frac{16\pi\sigma^3 T_m^2}{3(\Delta T)^2 (\Delta_{cr}H_V)^2 kT}\right] \tag{2}$$

where N_s is the number of adjacent particles, k is the Boltzmann’s constant, T is the thermodynamic temperature, h is the Planck’s constant, ΔG_a is the kinetic barrier to nucleation, N is the number of particles per unit melt volume, σ is the surface tension, T_m is the equilibrium melting temperature, $\Delta_{cr}H_V$ is the crystallization enthalpy per unit volume, and the undercooling ΔT is defined as:

$$\Delta T = T_m - T. \tag{3}$$

Supposing the temperature independent value of σ and $\Delta_{cr}H_V$ and merging together the constant terms the temperature dependence of homogeneous nucleation rate can be expressed by using three constant terms:

$$I(T) = K_I T \exp\left(-\frac{A_I}{T}\right) \exp\left[-\frac{B_I}{T(\Delta T)^2}\right], \tag{4}$$

where

$$K_I = \frac{N_s k N}{h} \tag{5}$$

$$A_I = \frac{\Delta G_a}{k} \tag{6}$$

$$B_I = \frac{16\pi\sigma^3 T_m^2}{3(\Delta_{cr}H_V)^2 k} \tag{7}$$

and $K_I, A_I, B_I > 0$.

Similarly the linear crystal growth rate can be expressed by [3, 16–19]:

$$u(T) = \lambda v_0 \exp\left(-\frac{\Delta G_a}{kT}\right) \left[1 - \exp\left(-\frac{\nu \Delta_{cr} H_m \Delta T}{V_m k T_m T}\right)\right], \tag{8}$$

where λ is the characteristic interparticle spacing, v_0 is the characteristic frequency of thermal particle vibrations, V_m is the molar volume, $\Delta_{cr}H_m$ is the molar crystallization enthalpy, and ν is the volume occupied by one particle. As in the case of the nucleation rate, we can express the temperature dependence of crystal growth by three constant parameters:

$$u(T) = K_u \exp\left(-\frac{A_u}{T}\right) \left[1 - \exp\left(-B_u \frac{\Delta T}{T}\right)\right], \tag{9}$$

where

$$K_u = \lambda v_0, \tag{10}$$

$$A_u = \frac{\Delta G_a}{k}, \tag{11}$$

$$B_u = \frac{\nu \Delta_{cr} H_m}{V_m k T_m} = \frac{\Delta_{cr} H_m}{R T_m}, \tag{12}$$

and $K_u, A_u, B_u > 0$

It is worth noting [16] that the activation barrier ΔG_a for growth and nucleation may not necessarily be equal, since the particle movements involved may be quite different for nucleation and growth.

Inserting Eqs. (4) and (9) into the Eq. (1) and supposing only the low values of the degree of conversion, α , we obtain:

$$V_{cr}(t) = K' \int_0^t T(t') \exp\left(-\frac{A_I}{T(t')}\right) \exp\left[-\frac{B_I}{T(t') [\Delta T(t')]^2}\right] \left\{ \int_{t'}^t \exp\left(-\frac{A_u}{T(t'')}\right) \left[1 - \exp\left(-B_u \frac{\Delta T(t'')}{T(t'')}\right)\right] dt'' \right\}^d dt', \tag{13}$$

where

$$K' = g K_I K_u^d V_{me}(0). \tag{14}$$

In case of higher degrees of conversion, the decreasing volume of melt has to be accounted by using the $-\ln[1 - \alpha(t)]$ instead of $V_{cr}(t)$ at the left hand side of the Eq. (13). Obviously the meaning of K' proportionality constant is correspondingly changed in this case.

Giving the set of values $\{K', A_I, B_I, A_u, B_u, d\}$, we can obtain the time dependence of V_{cr} by simple numerical integration of the Eq. (13) for an arbitrary time–temperature regime $T(t)$. If the experimental data $y^{\text{exp}}(t_i)$ proportional to $V_{cr}(t_i)$, i.e., $y^{\text{exp}}(t_i) = K_y V_{cr}(t_i)$, are measured then the least squares problem can be simply formulated:

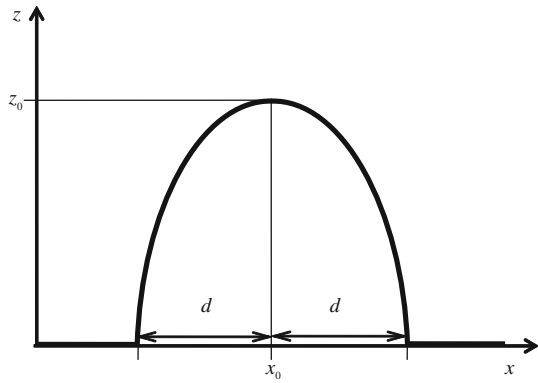


Fig. 1 The parabolic approximation used for growth and nucleation rates $-x = \Delta T = T_m - T$

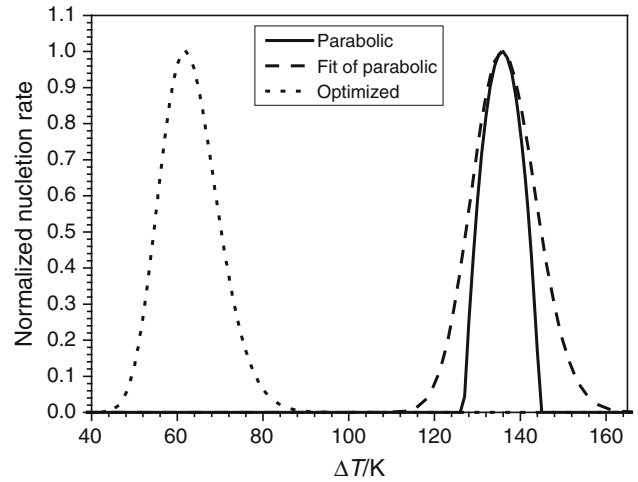


Fig. 3 Nucleation: α input data

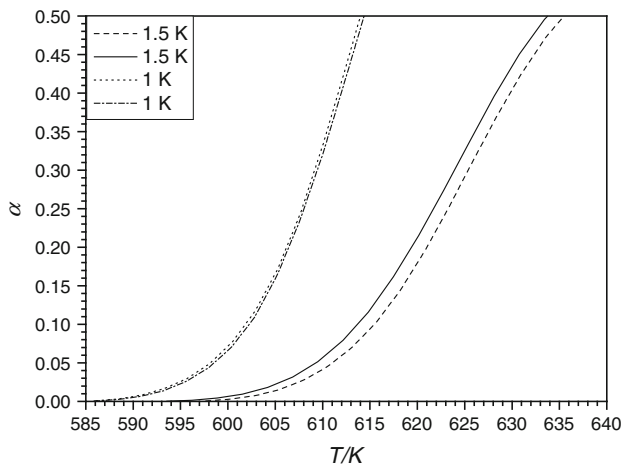


Fig. 2 Temperature dependence of conversion degree considered in the regression treatment

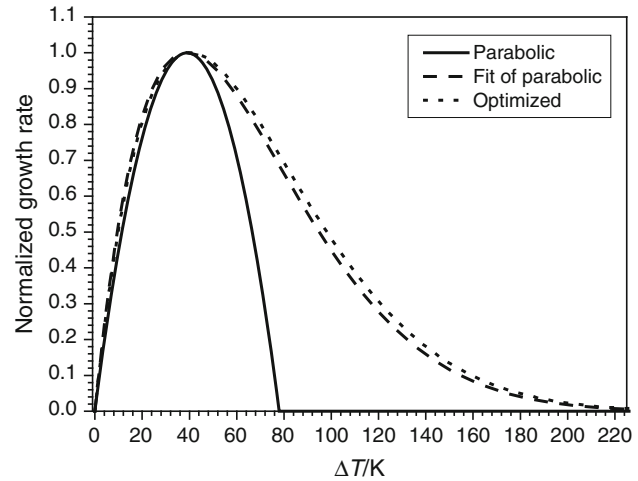


Fig. 4 Growth: α input data

Table 1 Parameters of quadratic approximation (16) of nucleation and growth rate temperature dependence (s_{apr} standard deviation of approximation)

Input data	x_{0l}/K	d_l/K	x_{0u}/K	d_u/K	$10^2 \cdot s_{apr}$
α	135.8 ± 0.1	9.0 ± 0.1	38.8 ± 1.0	39.3 ± 1.9	1.33
$-\ln(1 - \alpha)$	68.0 ± 2.8	9.1 ± 0.1	36.1 ± 5.8	49.0 ± 6.9	1.47

$$\begin{aligned}
 S(K, A_I, B_I, A_u, B_u, d) &= \sum_i [y^{\text{exp}}(t_i) - K_y V_{\text{cr}}(t_i)]^2 \\
 &= \sum_i [y^{\text{exp}}(t_i) - y^{\text{clc}}(t_i)]^2 = \min.,
 \end{aligned}
 \tag{15}$$

where $K = K_y K'$, and we suppose that the proportionality constant is known. However, this nonlinear least squares problem needs the appropriate starting estimates of the unknown parameters. These can hardly be found by simple mapping the sum of squares value as a function of six independent parameters. Even if only five parameters can be treated if we suppose some particular d value (e.g., $d = 3$), it is very difficult to cope with the problem due to existence of many local minima of S .

Table 2 Results of nonlinear regression analysis with theoretical growth (Eq. 9) and nucleation (Eq. 4) rates

Input data	$\log(A_I/K)$	$\log(B_I)$	$\log(A_u/K)$	$\log(B_u)$	$10^2 \cdot s_{apr}$
α	5.182 ± 0.047	7.508 ± 0.063	3.976 ± 0.040	0.081 ± 0.377	1.40
$-\ln(1 - \alpha)$	5.414 ± 0.001	7.785 ± 0.001	4.039 ± 0.001	-0.717 ± 0.001	2.03

See also Figs. 3, 4, 5, and 6

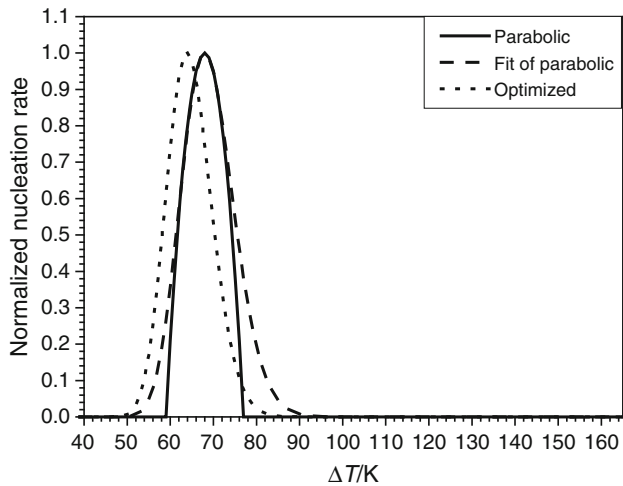


Fig. 5 Nucleation: $-\ln(1 - \alpha)$ input data

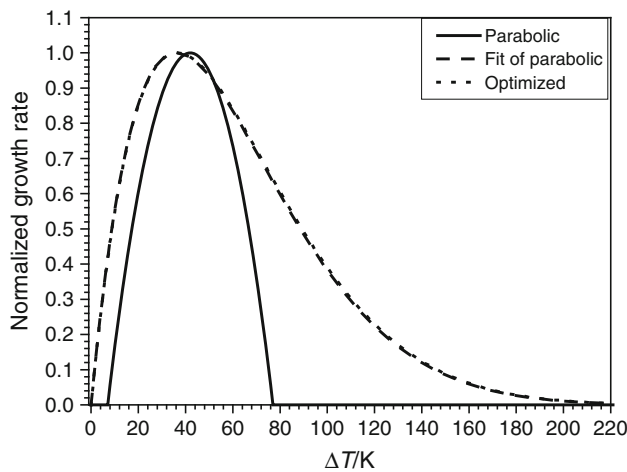


Fig. 6 Growth: $-\ln(1 - \alpha)$ input data

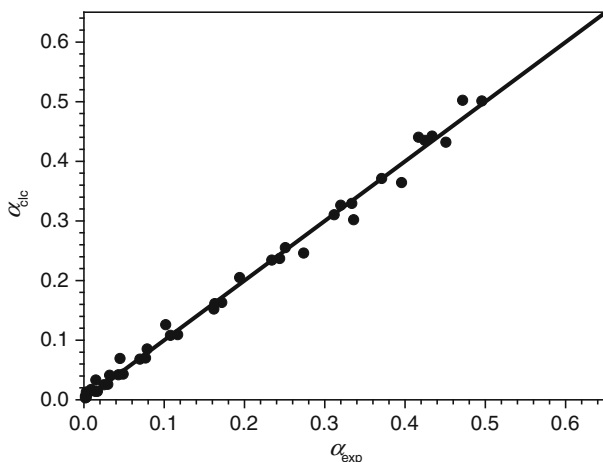


Fig. 7 Calculated versus experimental values for α input data

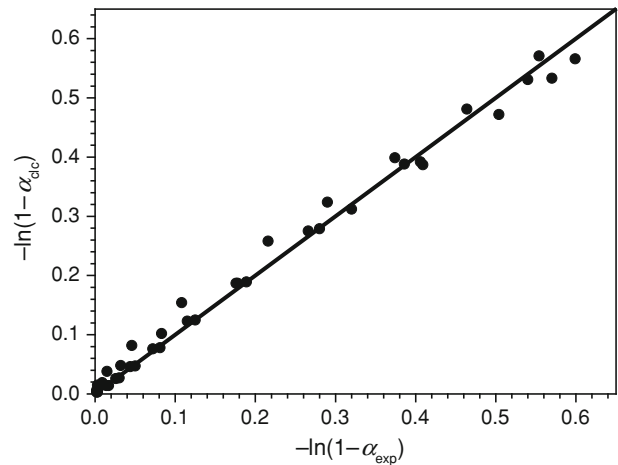


Fig. 8 Calculated versus experimental values for $-\ln(1 - \alpha)$ input data

To solve the above problem, we suggested in the first step the replacement of $I(T)$ and $u(T)$ functions by simple parabolic functions defined by:

$$z = \max \{0; a_z x^2 + b_z x + c_z\}; \quad x = \Delta T = T_m - T \geq 0, \tag{16}$$

where z stands for I or u . However in the regression analysis instead of parameters $a_z, b_z,$ and c_z are used parameters with simple physical meaning, i.e., the ΔT coordinate of the z maximum, x_{0z} , the maximal z value, z_{0z} , and the distance, d_z , from x_0 to x where z reaches the zero value, i.e., the basement half width of z (see Fig. 1). The following relationships are used for obtaining of $a_z, b_z,$ and c_z from $x_0, d,$ and z_0 .

$$a_z = -z_0/d_z^2 \tag{17}$$

$$b_z = 2z_0x_{0z}/d_z^2 \tag{18}$$

$$c_z = z_0 \left(1 - \frac{x_{0z}^2}{d_z^2}\right). \tag{19}$$

Thus in the first step, we use the parabolic approximations of I and u in the regression treatment of experimental data $y^{\text{exp}}(t_i)$. The Eq. (13) is evaluated with the K' constant set to one for this purpose:

$$y^{\text{red}}(t) = \int_0^t \left(a_1(\Delta T(t'))^2 + b_1\Delta T(t') + c_1 \right) \left\{ \int_{t'}^t \left[a_u(\Delta T(t''))^2 + b_u\Delta T(t'') + c_u \right] dt'' \right\}^3 dt'. \tag{20}$$

Because all multiplicative constants are cumulated into one constant, K_{par} we can set $u_0 = I_0 = 1$ and optimize only the values of $x_{0I}, x_{0u}, d_{0I},$ and d_{0u} . Moreover, we set $d = 3$ for As_2Se_3 crystallization.

For each set of $x_{0I}, x_{0u}, d_{0I},$ and d_{0u} values the value of K_{par} is obtained by one step linear regression from:

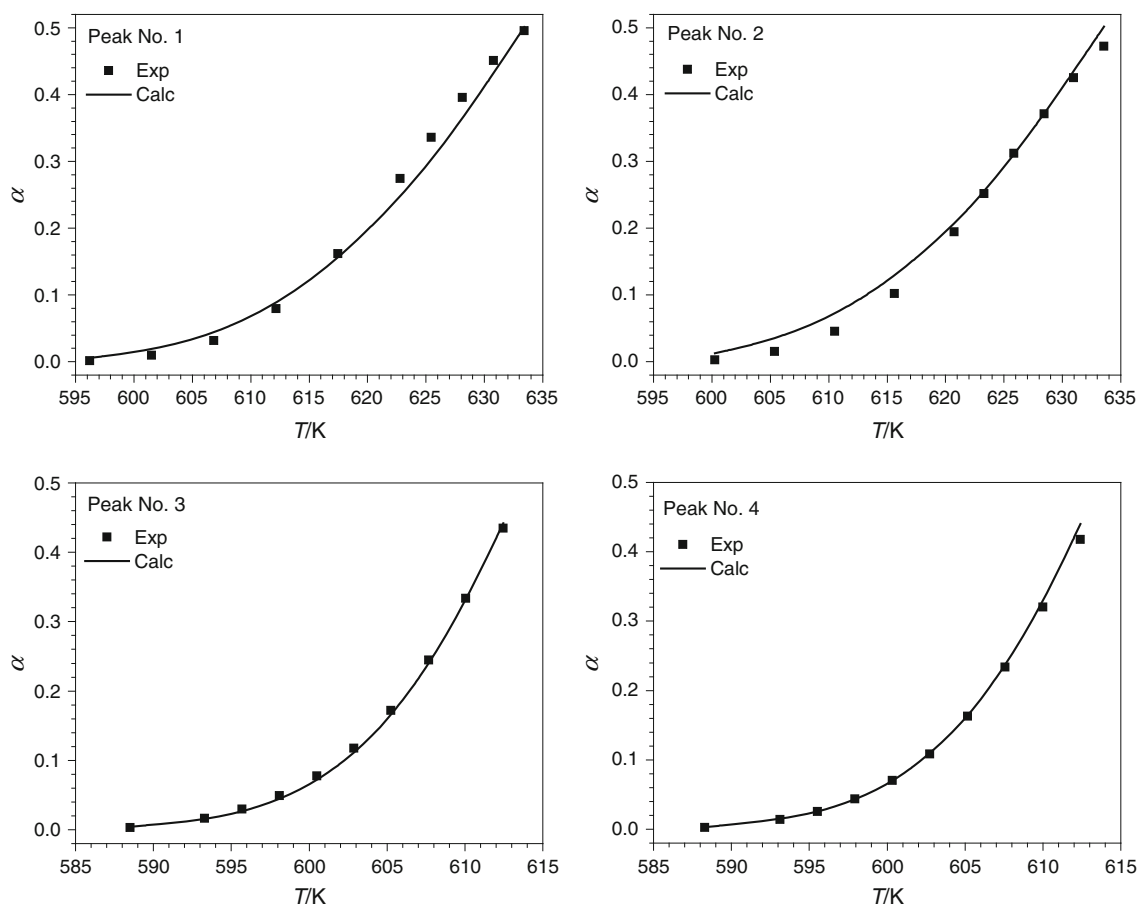


Fig. 9 Calculated curve versus experimental points for α input data (heat rate is 1.5 K min^{-1} for peak No. 1 and No. 2; 1.0 K min^{-1} for peak No. 3 and No. 4, $\alpha < 0.5$)

$$K_{\text{par}} = \frac{\sum_i y^{\text{exp}}(t_i) y^{\text{red}}(t_i)}{\sum_i [y^{\text{red}}(t_i)]^2}. \quad (21)$$

In the second step, the obtained optimal parabolic functions (with maximum value $u_0 = I_0 = 1$) will be fitted by standard nonlinear least squares method with the theoretical functions given by Eqs. (4) and (9). Such way the starting estimates of A_1 , B_1 , A_u , B_u needed for nonlinear least squares treatment of experimental data will be obtained.

In the last step, the nonlinear regression analysis of experimental data will be performed based on the theoretical (according the CNT) courses of $I(T)$ and $u(T)$ functions. The value of K' will be obtained in each step analogically to the previous treatment of the K_{par} constant.

Experimental

The As₂Se₃ glass was prepared by conventional direct synthesis (melt-quenching technique) from high purity elements (semiconductor purity—5 N elements). Synthesis was carried out in evacuated silica ampoules at $850 \text{ }^\circ\text{C}$ for

24 h in a horizontal rocking furnace in order to ensure the homogeneity of the melt. The melt was subsequently quenched in cold water. Both homogeneity and composition were controlled using X-ray fluorescence (XRF) analyzer Eagle II (Roentgen Messtechnik AG).

Four crystallization experiments consisting from three parts were realized. First the sample was heated from the room temperature by the constant heating rate of $5 \text{ }^\circ\text{C min}^{-1}$ to the nucleation temperature of $230 \text{ }^\circ\text{C}$. Then the isothermal nucleation of 60 min followed. After that the crystallization peak was recorded under the constant heating rate up to $385 \text{ }^\circ\text{C}$. The heating rates of $1.5 \text{ }^\circ\text{C min}^{-1}$ (peak No. 1 and 2) and $1.0 \text{ }^\circ\text{C min}^{-1}$ (peak No. 3 and 4) were used. The degree of conversion α was calculated from the relative peak area. Only the values $\alpha < 0.5$ were used in the subsequent regression treatment (Fig. 2). For the upper limit of such defined conversion degree region, the transformed function accounting for the decreasing volume of un-crystallized glass is significantly different from the α value, i.e., $-\ln(1 - 0.5) = 0.693$. Therefore, the regression treatment was performed at the transformed data too. The sum of squares of deviations

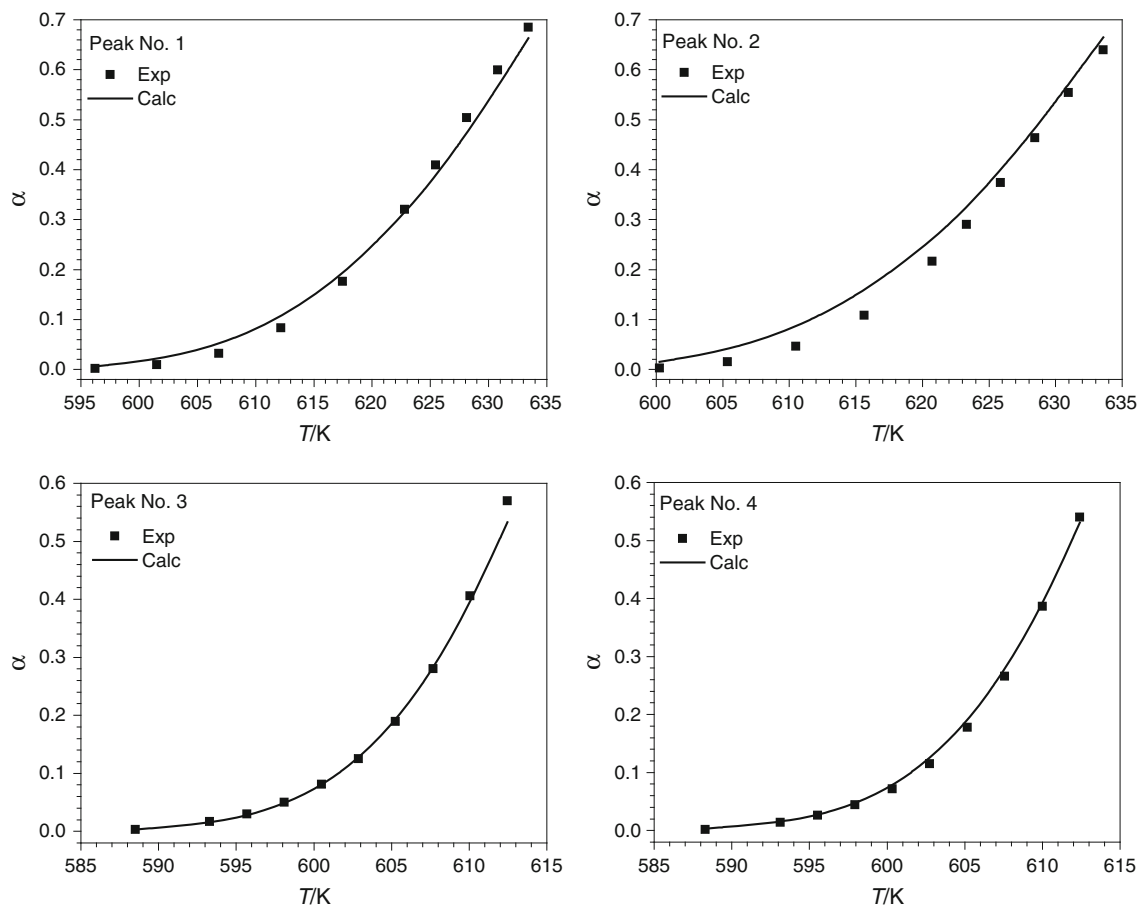


Fig. 10 Calculated curve versus experimental points for $-\ln(1 - \alpha)$ input data (heat rate is 1.5 K min^{-1} for peak No. 1 and No. 2; 1.0 K min^{-1} for peak No. 3 and No. 4, $\alpha < 0.5$)

containing the experimental data of all four measured crystallization peaks was minimized.

Results and discussion

The values of parameters of the parabolic I and u functions resulted for α and $-\ln(1 - \alpha)$ input data in the first step are summarized in Table 1.

Significant differences between the results obtained for transformed and untransformed input data can be seen mainly in the position of the nucleation maximum. The other parameters are within the standard errors practically equivalent.

In the second step, these fixed parabolic functions were least squares fitted (using the MS OFFICE-EXCEL Solver utility) by theoretical functions according to the Eqs. (4) and (9).

These parameters were in the last step used in the nonlinear regression treatment of experimental data by combination of the SIMPLEX method followed by the Pit mapping method [20]. The own written FORTRAN

program was used for calculation. In this step the logarithms of model parameters were optimized. Thus results summarized in the Table 2 are given in the logarithmic scale. It is worth noting that due to multiplicative mixing expressed by Eq. (14), the individual values of K_I and K_u are not determined. Therefore, we use for graphical presentation the functions normalized to unity maximum value.

From the results summarized in Table 2, it can be seen that both types of input data gave comparable results. In contrary to the results obtained in the work [15] the resulting $\log(A_I/K)$ values are higher than the values corresponding to the viscous flow activation energy [21]. In graphical form, the route from optimum quadratic functions to the optimum theoretical expressions can be found in Figs. 3, 4, 5, and 6. When comparing with the quadratic approximation (Figs. 4, 6) the extended non-zero low temperature tail is present in the optimum theoretical growth rate. In contrary (Fig. 5), the quadratic and theoretical courses are close for the nucleation rate obtained from $-\ln(1 - \alpha)$ input data. In case of α input data, the quadratic approximation of nucleation rate (Fig. 3) is

shifted to unrealistically high undercooling values. The preferable use of $-\ln(1 - \alpha)$ input data is implied by this fact. Comparing visually Fig. 3 with Fig. 5 and Fig. 4 with Fig. 6, it can be found that the resulting optimized theoretical growth and nucleation rate temperature dependences are almost identical for α and $-\ln(1 - \alpha)$ input data. The calculated and experimental values are graphically compared in Figs. 7 and 8. It can be seen that the experimental data are described with acceptable accuracy in both cases.

In Fig. 9, we can see the calculated curves which are compared with experimental points for $\alpha < 0.5$ (heat rate for peak No. 1 and peak No. 2 is 1.5 K min^{-1} and for peak No. 3 and peak No. 4 it is 1.0 K min^{-1}). Figure 10 shows the same as the previous figure for $-\ln(1 - \alpha)$, $\alpha < 0.5$

Conclusions

The nonlinear regression analysis of conversion dependence on isothermal nucleation temperature and time was performed in frame of the classical nucleation theory supposing the normal 3D growth. It was found that the parameters of temperature dependence of nucleation rate and growth rate can be determined by proposed three step process. First, the simple parabolic model was used to estimate the maximum and width of rate temperature dependence. Then the obtained parabolic curves were fitted by the theoretical ones. In the third step, the obtained parameters were used in connection with the theoretical nucleation and growth rate curves for nonlinear regression analysis of experimental data. It was shown that for α values less than 0.5 the $-\ln(1 - \alpha)$ input data gave practically the same courses of nucleation and growth rate theoretical dependence. However, the use of $-\ln(1 - \alpha)$ input data is preferred. The resulted nucleation and growth curves fit the experimental data with acceptable accuracy. The kinetic barrier of crystal growth was found higher than the viscous flow activation energy.

Acknowledgments This work was supported by the Slovak Grant Agency for Science under the grant VEGA 1/0006/12 and the bilateral project SK-CZ-0007-11. This publication was created in the frame of the project ZDESJE, ITMS code 26220220084, of the Operational Program Research and Development funded from the European Fund of Regional Development. The Ministry of Education, Youth and Sports of the Czech Republic, Project CZ.1.07/2.3.00/30.0021 “Strengthening of Research and Development Teams at the University of Pardubice”, financially supported this work.

References

- Li W, Seal S, Rivero C, Lopez C, Richardson K, Pope A, Schulte A, Myneni S, Jain H, Antoine K, Miller AC. Role of S/Se ratio in chemical bonding of As-S-Se glasses investigated by Raman, X-ray photoelectron, and extended X-ray absorption fine structure spectroscopies. *J Appl Phys*. 2005;98:053503.
- Carlie N, Musgraves JD, Zdyrko B, Luzinov I, Hu J, Singh V, Agarwal A, Kimerling LC, Canciamilla A, Morichetti F, Melloni A, Richardson K. Integrated chalcogenide waveguide resonators for mid-IR sensing: leveraging material properties to meet fabrication challenges. *Optics Express*. 2010;18:26728–43.
- Varshneya AK. *Fundamentals of inorganic glasses*. Sheffield: Society of Glass Technology; 2006.
- Rao KJ. *Structural chemistry of glasses*. Amsterdam: Elsevier; 2003.
- Shaaban ER, Mohamed SH. Thermal stability and crystallization kinetics of Pb and Bi borate-based glasses. *J Therm Anal Calorim*. 2012;107:617–24.
- Wu X, Wu W, Cui X, Liao S. Preparation of nanocrystalline BiFeO₃ via a simple and novel method and its kinetics of crystallization. *J Therm Anal Calorim*. 2012;107:625–32.
- Svoboda R, Málek J. Extended study of crystallization kinetics for Se–Te glasses. *J Therm Anal Calorim*. 2013;111:161–71.
- Patel AT, Pratap A. Kinetics of crystallization of Zr₅₂Cu₁₈Ni₁₄Al₁₀Ti₆ metallic glass. *J Therm Anal Calorim*. 2012;107:159–65.
- Svoboda R, Málek J. Crystallization kinetics of amorphous Se. *J Therm Anal Calorim*. 2013;. doi:10.1007/s10973-012-2922-1.
- Pliško A, Liška M, Pagáčová J. Crystallization kinetics of Al₂O₃–Yb₂O₃ glasses. *J Therm Anal Calorim*. 2012;108:505–9.
- Koga N, Šesták J. Thermoanalytical kinetics and physico-geometry of the nonisothermal crystallization of glasses. *Boletín de la Sociedad Espanola de Ceramica y Vidrio*. 1992;31:185–90.
- Liška M, Holubová J, Chromčíková M, Černošková E, Jakubíková Z, Černošek Z. Raman spectra, structure and thermodynamic model of As₂S₃–As₂Se₃ glasses. *Phys Chem Glasses*. 2011;B52:1–6.
- Holubová J, Černošková E, Černošek Z. Nucleation of As₂Se₃ undercooled liquid. In: 32nd International Czech and Slovak seminar on calorimetry, University of Pardubice, Lísek u Bystřice nad Pernštejnem; 2010. p 185–8. ISBN: 978-80-7395-259-4.
- Holubová J, Černošek Z, Černošková E, Liška M. Glassy system As–S–Se. In: 28th International Czech and Slovak seminar on calorimetry, University of Pardubice, Pardubice; 2006. p 133–6. ISBN: 80-7194-859-4.
- Liška M, Holubová J, Černošková E, Černošek Z, Chromčíková M, Pliško A. Nucleation and crystallization of an As₂Se₃ undercooled melt. *Phys Chem Glasses*. 2012;53:289–93.
- Paul A. *Chemistry of glasses*. London: Chapman & Hall; 1982.
- Turnbull D, Cohen MH. Crystallization kinetics and glass formation. In: Mackenzie JD, editor. *Modern aspects of the vitreous state*. London: Butterworths; 1960. p. 38–62.
- Šesták J. *Heat, thermal analysis and society*. 1st ed. Hradec Kralove: Nukleus HK; 2004. p. 119–124, 126–132, 204–214. ISBN 80-86225-54-2.
- Šesták J, Koga N. Influence of preliminary nucleation on the physico-geometric kinetics of glass crystallization. *Thermal analysis of micro, nano- and non-crystalline materials. Hot topics in thermal analysis and calorimetry*, vol 9; 2013. p. 209–23.
- Dyrssen D, Ingri N, Sillen LG. “Pit-mapping”—a general approach for computer refining of equilibrium constants. *Acta Chem Scand*. 1961;15:694–6.
- Málek J, Šánělová J. Structural relaxation of As₂Se₃ glass and viscosity of supercooled liquid. *J Non-Cryst Solids*. 2005;351:3458–67.